A Novel Microdosimeter Based Upon Artificial Single Crystal Diamond

Sofia Rollet, Maurizio Angelone, Giulio Magrin, Marco Marinelli, Enrico Milani, Mario Pillon, Giuseppe Prestopino, Claudio Verona, and Gianluca Verona-Rinati

***Abstract*—This paper represents the first attempt to discuss the use of an artificial single-crystal diamond as a new microdosimeter. The Diamond MicroDosimeter (DMD) detecting region is a thin layer of highly controlled thickness ($< 5\ \mu\mathrm{m}$) and high purity intrinsic monocrystalline diamond grown over a backing boron doped monocrystalline diamond. This viable, small, compact and user-friendly device is able to obtain spectra of the energy deposition in sensitive volumes of the order of micrometer. The paper reports the first experimental tests performed to measure the dose distribution in terms of lineal energy and the simulation performed by the Monte Carlo code FLUKA to optimize the design of the new DMD. Advantages and shortcomings of the DMD are discussed.**

***Index Terms*—Artificial single crystal diamond detector, diamond microdosimeter, microdosimetry, Monte Carlo simulation.**

I. Introduction

ARTIFICIAL diamond detectors have been studied for many years, however recently there has been a boost in their use thanks to the development of high quality single crystal diamonds mainly produced by the chemical vapor deposition (CVD) technique [1]–[4].

Diamond detectors have been tested and used in many fields, including high energy physics, to estimate the effects of charged particles, both fast and thermal neutrons, UV and soft X-rays etc. [4]–[8]. This wide range of applications is possible thanks to the many outstanding diamond properties [9] such as high band gap, high resistivity, good energy resolution (FWHM $< 0.4\%$ measured using 5.5 MeV alphas [6]), radiation hardness, and capability to operate at high temperature which make diamond a very attractive material for radiation detection. One more interesting property of diamond so far not fully exploited, relates to its atomic number $(Z = 6)$. For radiation interactions carbon is a material similar to human tissue counting on average for 18% of body weight and being close, in atomic number, to oxygen. However, dosimetry with diamond is not straightforward also because the diamond density $(3.52\ \mathrm{g\ cm^{-3}})$ is not the same as that of tissue, the latter being close to unity. Basic dosimetric concepts, such as the equivalence of stopping powers between tissue and tissue-equivalent materials, allow bypassing this problem.

Due to the above characteristics diamond dosimeters are widely investigated and proposed for medical and environmental applications. These existing or proposed applications have so far included in-phantom measurement of X-ray and gamma doses, thermoluminescence, measurement of Ambient dose Equivalent $(\mathrm{H}*)$ and hadron therapy [10], [11] but, in the authors knowing, no attempt to use diamond in microdosimetric measurements have been reported yet.

This paper represents the first effort to propose and discuss, with experiments and simulations, the use of synthetic single-crystal diamond as a new microdosimeter (DMD). Such a detector allows the direct measurement of the energy deposited in a single event at a microscopic level. This can be used to measure the quality of radiation, i.e., to set apart sparsely ionizing from densely ionizing radiation. In radiotherapy, the beam quality is usually calculated, hence such a device, capable of measuring the resulting radiation damage in biological matter, can be a valuable tool. In comparison with a standard Tissue Equivalent Proportional Counter (TEPC), the DMD has faster charge collecting time and can be made with smaller cross section, reducing the signal pile-up encountered at the typical hadron therapy beam intensities. Moreover, the device is drastically simplified since there is no need of managing gas flux and the polarization voltage is in the range of volts instead of kilovolts. These characteristics make the diamond microdosimeter a convenient, manageable and user-friendly detector for hadron therapy.

Since the novel DMD has a thickness of a few micrometers the polarization can be provided by a simple battery, with the advantage of reducing the electronic noise and make it easily portable. Furthermore, since this detector is characterized by the presence of a Schottky junction it can also be operated without the need of an external bias. Therefore, the DMD can also be used in the complex radiation fields present in space environment as well as in nuclear waste management and other industrial fields with limited accessibility, remote operation and low maintenance requirements. Although the use of diamonds for microdosimeteric measurements has been already suggested providing simulations [12], this article represents the first experimental collection of microdosimetric data using CVD diamond.

Manuscript received December 14, 2011; revised March 23, 2012; accepted July 10, 2012. Date of publication September 06, 2012; date of current version October 09, 2012.

S. Rollet is with the AIT-Austrian Institute of Technology, Donau-City-Strasse1-1220 Vienna, Austria (e-mail: sofia.rollet@ait.ac.a).

M. Angelone, M. Pillon, and G. Prestopino are with the Associazione Euratom-ENEA sulla fusione, ENEA C.R. Frascati, CP 65, I-00044 Frascati, Italy (e-mail: maurizio.angelone@enea.it; Mario.Pillon@enea.it; giuseppe.prestopino@uniroma2.it).

G. Magrin is with the EBG MedAustron, Viktor Kaplan-Straße 2, A-2700 Wiener Neustadt, Austria (e-mail: giulio.magrin@medaustron.at).

M. Marinelli, E. Milani, C. Verona, and G. Verona-Rinati are with the Università degli Studi "Tor Vergata" Rome, Department of Mechanical Engineering. Via del Politecnico, 1-00100 Roma, Italy (e-mail: milani@uniroma2.it; marco.marinelli@uniroma2.it; claudio.verona@uniroma2.it; gianluca.verona.rinati@uniroma2.it).

Color versions of one or more of the figures in this paper are available online at http://ieeexplore.ieee.org.

Digital Object Identifier 10.1109/TNS.2012.2209677

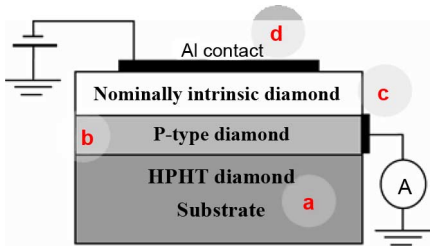

Fig. 1. Schematic representation of the detector. Sizes are not proportional to real dimensions.

II. Background

A. Reference Quantities and Comparison With Standard Detectors

In microdosimetry it is fundamental to measure the imparted energy ε, the derived quantity lineal energy y, as well as their distributions in volumes which are of the order of a mammalian cell nucleus (a few micrometers in diameter). The lineal energy y is defined as the energy imparted in a single event within this volume divided by the mean chord length l of the volume itself, i.e., $\mathrm{y} = \varepsilon/l$. The lineal energy evaluated from microdosimetric measurements is represented in form of pulse-height distributions, i.e., microdosimetric spectra, which can be used to evaluate the quality of a radiation [13], [14].

The reference microdosimeters are the TEPCs proposed by H.H. Rossi in the fifties [15] in which detectors of several centimeters of diameter filled with gas, simulate tissue of micrometric sizes at density close to unity.

Several attempts have been made and are still ongoing to use silicon based microdosimeters, however the non-tissue equivalence and the intrinsic noise due to the p-n junction are important drawbacks [16]–[18].

A microdosimeter can measure the distribution of lineal energies in complex radiation fields [19], providing the possibility of estimating biological effects of ionizing radiations by analyzing the different spectra [20]. Solid-state microdosimeters can become an important alternative to traditional ones in specific applications including radiation protection and radiation therapy. They exhibit a substantial reduction of detector active volume, the absence of complex gas-flow systems, low-voltage polarization, and no wall-effect distortion [21] since the sensing volume is solid.

B. Monocrystalline Diamond With Micrometric Sensitive Volumes

The availability of high quality Single Crystal Diamonds (SCD) fabricated with a layered structure [4] and produced at Rome "Tor Vergata" University has led to the realization of the new DMD. The detector is based on a layered structure built in cascade (Fig. 1). This is obtained by first growing a high boron doped monocrystalline film which works as backing contact on top of a low-quality and low cost commercial high pressure high temperature (HPHT) diamond used as lattice base (a in Fig. 1). In a second step, a high quality single crystal diamond of variable thickness (active region, c in Fig. 1) is grown on top of the p-doped diamond layer (b in Fig. 1). Finally, an aluminum contact is deposited by thermal evaporation on top of the active region which forms a Schottky metal-diamond barrier (d in Fig. 1). This detector is thus characterized by the presence of a Schottky junction with a built-in potential of about 1.5 eV so that it can also operate without the need of an external bias. Details of the detector are addressed elsewhere [4], [22].

The main advantage of such a detector is the possibility of growing very thin layers of high purity intrinsic single crystal diamond with a high capability to control their thickness. The first test of the new DMD was performed using neutrons and alpha particles.

III. Experimental Set-up

The experimental set-up is composed by a standard power supply unit, a commercial charge preamplifier (ORTEC 142A), a commercial amplifier (ORTEC 572) and a multichannel analyzer (ORTEC 919) for the collection of the pulse height spectra (PHS). The readout system has a shaping time of 2 μs and noise lower than 20 mV. The amplification gain was set to 100. The measurements were performed using two diamond detectors with nominal thicknesses of 2 μm and 4 μm and contacted with a 2 mm diameter aluminum electrode 100 nm thick. The detectors are housed in an aluminum casing equipped with an SMA connector. The working biasing was 6 V and 15 V for the 2 μm and 4 μm thick detectors respectively. However, tests using just the built-in potential were also performed showing that the detector can properly operate without external bias.

In these preliminary tests the transversal shape of the sensitive volume was not geometrically defined by the electrodes and an aluminum collimator (2.5 mm diameter) has been used to restrict the volume of interaction.

IV. Numerical Simulations

Detailed models of the experimental setups were produced via Monte Carlo FLUKA code [23], [24].

The simulations of the DMD response are performed with two aims: first to study the characteristics of the distribution of the pulse heights for different detector characteristics in particular versus the diamond thicknesses (region *c, see* Fig. 1), and second to guide the experimental tests to the self calibration of the detector.

As a preliminary check, only the essential parts of the experimental assembly were simulated. The thin diamond layers (1.35, 2, 3, 4, 5, 6 μm thickness) on top of the diamond substrate (400 μm thickness) were both described in the FLUKA geometry as cylinders of different diameters (2 and 4 mm, respectively). The thin aluminum contact on top was also simulated (100 nm thickness), but it had no significant effects on the response (the 5.5 MeV alpha loses < 15 keV in it). An aluminum collimator, enclosing the diamond, was simulated with different collimator hole diameters (2, 3, 4, 5, 6, 7 mm).

The primary use of the collimator is to limit the distortions of the collected spectra due to particles that cross the sensitive volume not perpendicularly to the face of the detector. In fact, presently the sensitive volume is far from being as regular as in TEPCs which are either spherical or cylindrical with identical height and diameter, and therefore can not be used in isotropic

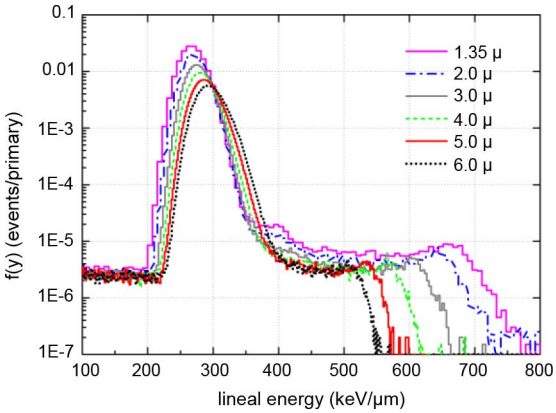

Fig. 2. Simulated frequency distribution of pulse heights of a $^{241}\mathrm{Am}$ alpha source in diamond (thicknesses 1.35, 2, 3, 4, 5 and 6 $\mu\mathrm{m}$).

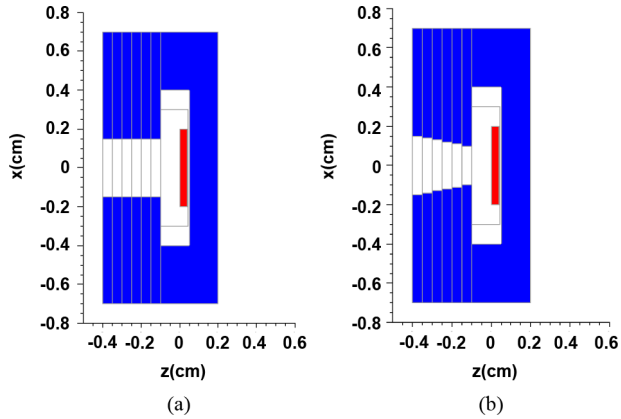

Fig. 3. Fluka geometry showing the Al casing and two different types of collimators: (a) cylindrical and (b) conical.

radiation. As will be shown in Section V, the presence of a collimator and its partial interaction with the alpha particles also has an important role in the calibration of the detector and in general to confirm the physical interpretation of the results. The collimator could also be used as a fast way to defining the transversal size of the sensing volume. For these reasons an accurate simulation study has been performed to investigate the influence of the collimator geometry on the results.

The source distribution was assumed to be forward directed with a 500 mrad gaussian angular distribution and momentum distribution with 8% FWHM. In a set of preliminary simulations, the irregular edge of the collimator, the backscattering from the surrounding structure, and the B-doped layer were not considered. A cylindrical aluminum collimator with a fixed thickness of 3 mm and aperture hole of 3 mm diameter was considered.

The response of the detector to a $^{241}\mathrm{Am}$ alpha source ($\mathrm{E}_\alpha = 5.5\ \mathrm{MeV}$) was simulated. The number of events per primary particle emitted from the source in the detector layer as a function of lineal energy is shown in Fig. 2.

Each curve in the figure is calculated with a different diamond thickness from $1.35\ \mu\mathrm{m}$ up to $6\ \mu\mathrm{m}$. The main peak of the distribution expresses the most probable energy deposition and depends on the particles energy and on the mean path crossed by the particles on the sensitive volume. The maximum lineal energy corresponding to this peak in the distribution can be estimated from the table of the range of alpha particles in carbon available in literature [25].

All the curves are already corrected dividing the energy deposition events by the proper thickness; the peaks slightly shift to the right with increasing thicknesses due to the increasing stopping powers. The distributions in Fig. 2 are represented in logarithmic scale so as to emphasize the contribution of alpha particles stopped inside the detector having lost most of their energy in the surrounding materials. The maximum values of the lineal energy, clearly visible on the right side of the main peak, range from approximately 550 to $800\ \mathrm{keV}/\mu\mathrm{m}$, depending on detector thickness and form the "alpha edge" created by the particles that stop inside the detector just after crossing the largest chord of the sensitive volume.

The lineal energies of both peak and alpha edge depend on the sensing thickness in opposite ways. The lineal energy of the peak increases with increasing thickness while the lineal energy of alpha edge decreases. This gives the opportunity to estimate the real thickness of the sensitive volume matching experimental data with simulation at the two lineal energy values of interest.

A new set of simulations is then done taking into account the real geometry of the diamond substrate ($4 \times 4 \times 0.4\ \mathrm{mm}^3$ in size), the aluminum contact and the thin sensitive layer as well as the aluminum box surrounding the detector, as shown in Fig. 3. Two types of collimators were considered, one with a constant cylindrical section (Fig. 3(a)) and one with a conical shape of decreasing diameter (Fig. 3(b)).

The $^{241}\mathrm{Am}$ alpha particles lose energy scattering with the aluminum collimator and, starting from the 5.5 MeV energy peak produce a long tail of particles at lower energies, as shown in Fig. 4. The collimator shape has a strong influence on the energy spectra due to the increasing scattering of the particles with the walls. This is evidenced comparing the energy spectra for a cylindrical shaped hole (geometry represented in Fig. 3(a) and spectrum in Fig. 4(a)) and for a conical shaped hole (geometry represented in Fig. 3(b) and spectrum in Fig. 4(b)). The ratio between the number of events in the peak and in the tail can change more than one order of magnitude, considering also a shift of the collimator center in the x and y directions.

Together with the collimator shape it is important also to consider the aperture of the collimator hole. As shown in Fig. 5 the ratio between the number of events that fall on the main peak and on the alpha edge region decreases as the diameter decreases but without changing the corresponding lineal energies.

This result shows how, for alpha irradiation, a collimator can be used as a way to increase the tail at lower energies components so as to emphasize the alpha edge maintaining the peak at the same lineal energy value.

During the experiment, the alpha edge was not generated reducing the collimator hole diameter but moving off axis the collimator. This shift was simulated with a full set of Monte Carlo calculations whose results are reported in Fig. 6.

All the previous calculations were done for source and detector in vacuum. The presence of air simply shifts the main

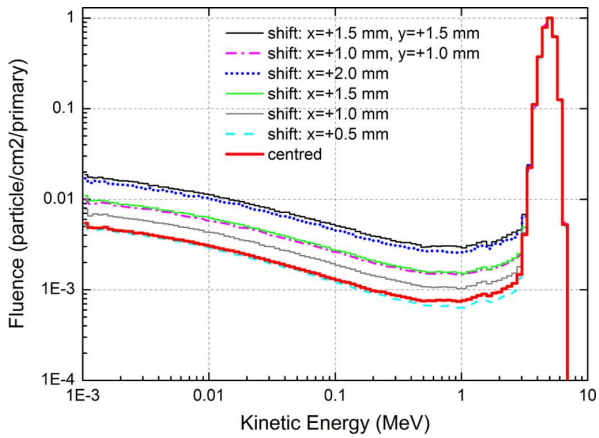

(a)

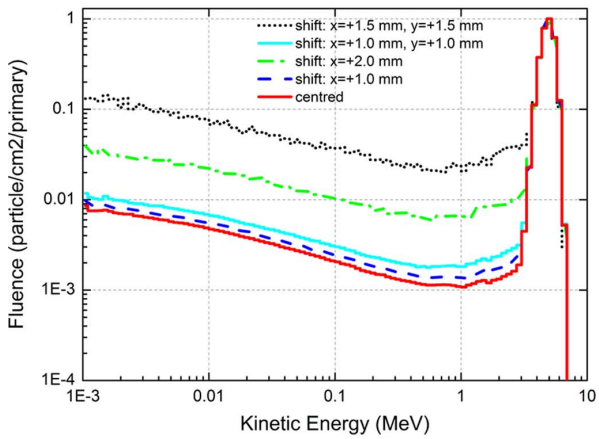

(b)

Fig. 4. Energy spectra from a $^{241}\mathrm{Am}$ alpha source in the diamond detector with cylindrical (a) and conical (b) collimator.

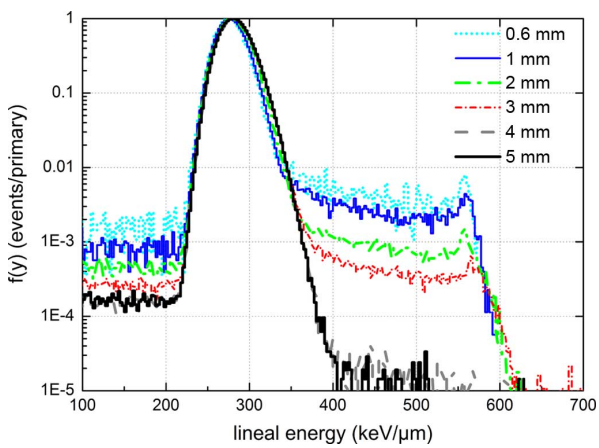

Fig. 5. Simulated frequency distribution of pulse heights of a 241Am alpha source in diamond for different collimator diameters (0.6, 1, 2, 3, 4 and 5 mm).

peak to higher lineal energy, without changing the contribution from the "stoppers" at the alpha edge, as shown in Fig. 7. This emphasizes the sensitivity of the detector to small variations of the source energy. The effect of the Al casing is negligible.

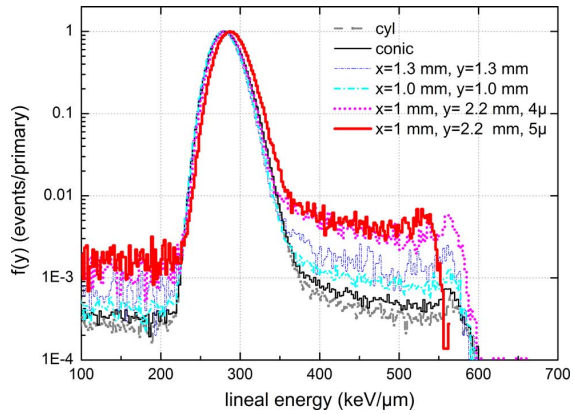

Fig. 6. Simulated frequency distribution of pulse heights of a 241Am alpha source in diamond for different collimator shapes and displacements from the center position.

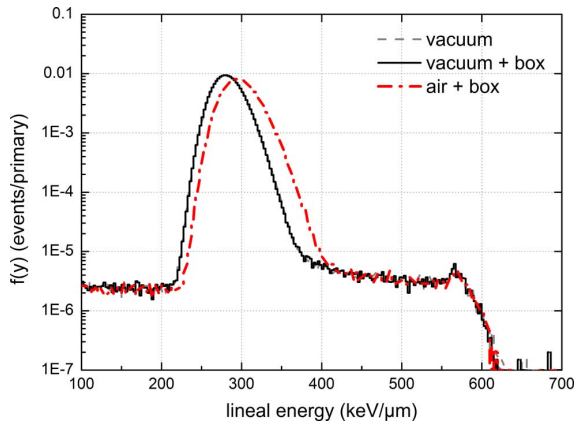

Fig. 7. Simulated frequency distribution of pulse heights of a $^{241}\mathrm{Am}$ alpha source in diamond (thickness 4 μm) with and without air.

V. Alpha and Neutron Measurements

A series of tests with alpha sources have been performed to evaluate the response of the detector to the different electronics setups and source characteristics.

A $^{241}\mathrm{Am}$ alpha source (primary energy 5.48 MeV and alpha emission 84.5%) was used for a first check.

Based on the simulations discussed in the previous section, the first part of the experimental investigation was dedicated to evaluate the actual thickness of the sensitive volume (c, see Fig. 1). Knowing the thickness of the sensitive volume is fundamental for determining with accuracy the mean and the maximum chord length and, consequently, for the calibration of the detector in linear energy. Although the metrology tests can precisely evaluate physical sizes of the diamond layers, the active thickness has an intrinsic imprecision, being defined by the depletion layer thickness below the metal contact plus diffusion length of carriers generated close to the depleted region [17].

From the simulated frequency distribution of pulse heights of a $^{241}\mathrm{Am}$ alpha in diamond (Fig. 2), it is possible to calculate the ratio between the lineal energies at the edge and at the peak as a function of diamond thickness. The corresponding data are shown in Fig. 8, where the dashed line represents the linear best fit of the diamond thickness. The lineal energy ratio of edge and

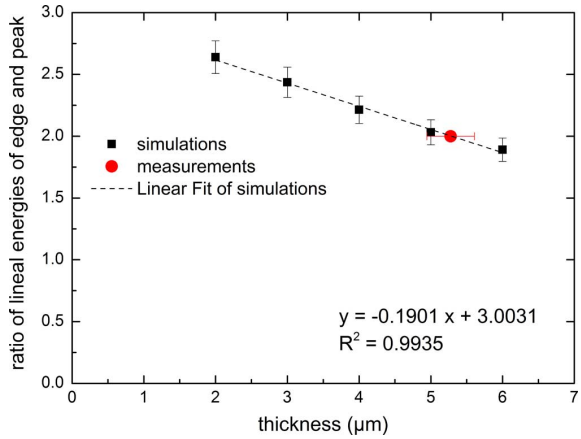

Fig. 8. Correlation between the ratio of the lineal energies of edge and peak and diamond thickness. The linear fit (dashed line) of the values obtained at different simulated thickness (squares) is used to evaluate the actual thickness of the diamond using the values (edge and peak) extracted from experimental microdosimetric spectrum.

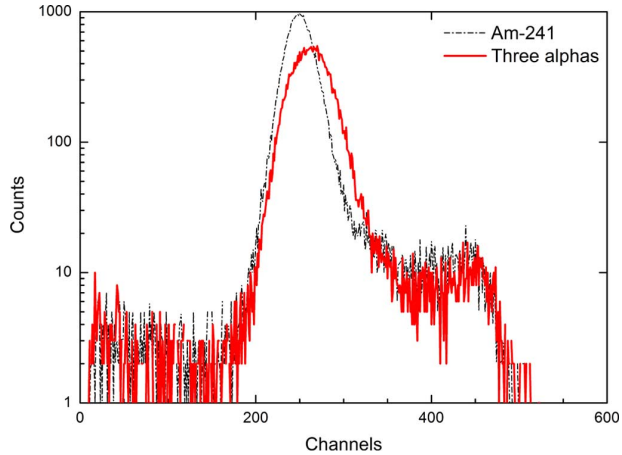

Fig. 10. Output of the multichannel analyzer for a diamond detector exposed to alpha particle from a $^{241}\mathrm{Am}$ source and a $^{239}\mathrm{Pu} + ^{241}\mathrm{Am} + ^{244}\mathrm{Cm}$ three alpha peaks source.

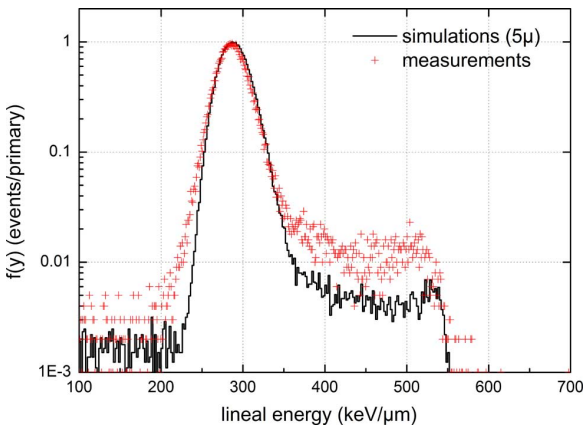

Fig. 9. Comparison between simulated and measured frequency distribution of pulse heights of a $^{241}\mathrm{Am}$ alpha in diamond (simulated thickness $5\ \mu\mathrm{m}$).

peak of the measured distribution is shown in the same picture. The actual thickness of the diamond sensing volume is calculated using the best fit parameters obtained with the simulation. A 5% uncertainty is assumed for each simulated ratio, the uncertainty on the actual diamond thickness is calculated from the experimental uncertainty estimated for the lineal energy values of peak and edge. The estimated thickness of the detector, $c = 5.3 \pm 0.3\ \mu\mathrm{m}$, is not incompatible with the nominal thickness of 4 ± 1 estimated during the diamond production.

Fig. 9 shows the comparison between measured and simulated data when the complete geometry of the experimental system is taken into account. As described in the previous session, the highest non-zero channel identifies the alpha edge and represents the maximum energy that can be deposited by an alpha particle in the sensitive volume, giving the possibility of calibrating the spectra in terms of lineal energy [13]. Considering the $5\ \mu\mathrm{m}$ thickness, the alpha edge of measurements and simulations coincide around $550\ \mathrm{keV}/\mu\mathrm{m}$.

The position of the collimator, and its shape, are highly effective in increasing the number of particles interacting. As shown in Figs. 5 and 6, collimator displacements of the order of 1 mm could result in doubling the number of events in the interval $380-550\ \mathrm{keV}/\mu\mathrm{m}$. The position of the edge, instead, is strongly correlated to the diamond thickness and changes only very little with the collimator geometry. Therefore, the displacement of the aluminum collimator is used to 'artificially' increase the relative number of events in the edge's region, without affecting its position. In Fig. 9 the excess of events measured compared to those calculated by the numerical simulations in the interval $380 - 550\ \mathrm{keV}/\mu\mathrm{m}$ can be explained by a small discrepancy $(< 1\ \mathrm{mm})$ between the simulated position of the collimator compared to the real one. Hence, the number of particles that interact with the collimator is slightly larger. Nevertheless, this effect will not interfere during the normal operation of the detector as microdosimeter: the displacement of the collimator is only used for calibration purposes and for determining the volume sensing thickness. During normal operation the collimator will be centered with the detector sensing volume and the spectra collected will be similar to those simulated in Fig. 5 for the 5 mm curve.

Further experimental studies resulted in a first evaluation of the detector sensitivity by measuring the variation of the lineal energy of the peak of two different alpha energies, 5.48 MeV from $^{241}\mathrm{Am}$ and 5.15 MeV from $^{239}\mathrm{Pu}$. A commercial $^{239}\mathrm{Pu} + ^{241}\mathrm{Am} + ^{244}\mathrm{Cm}$ source (alpha energies of 5.15, 5.48 and 5.78 MeV respectively) with a total activity of 5.5 kBq available in our laboratory was used for this purpose [26]. The lineal energy of the peak of plutonium was estimated indirectly from the data of a three-peak alpha source, formed by $^{239}\mathrm{Pu}$, $^{241}\mathrm{Am}$, and $^{244}\mathrm{Cm}$ sources with relative activities of 50%, 33%, and 17% respectively.

The frequency distribution of plutonium and curium components was obtained subtracting from the distribution of the triple source displayed in Fig. 10 the contribution of americium source conveniently scaled taking into account its relative activity. The peak in this distribution is essentially due to $^{239}\mathrm{Pu}$ given the lower activity of the $^{244}\mathrm{Cm}$ and the higher energy of its alpha particles. The increase of the peak lineal energies, estimated from the experimental data is $\Delta \mathrm{y}_{\mathrm{peak\,exp}}(^{241}\mathrm{Am}, ^{239}\mathrm{Pu}) = 11.9\ \mathrm{keV}/\mu\mathrm{m}$. This result can be compared with the value $\Delta \mathrm{y}_{\mathrm{peak}}(^{241}\mathrm{Am}, ^{239}\mathrm{Pu}) =$

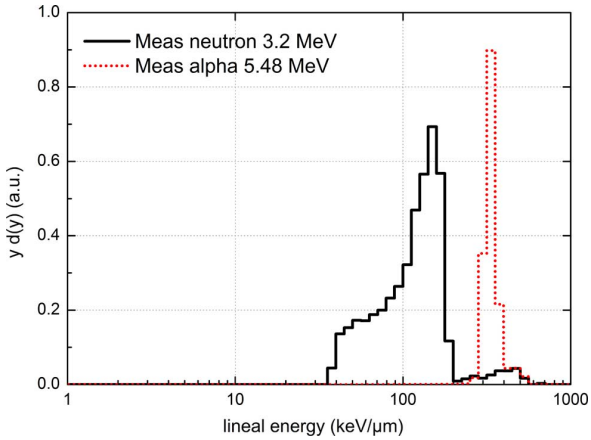

Fig. 11. Measured lineal energy distributions in the DMD for alpha (5.48 MeV) and neutron (3.2 MeV) (The curves are not normalized).

$8.6\ \mathrm{keV}/\mu\mathrm{m}$ estimated from data available on ranges and using the method described by Gerdung [27]

The discrepancy of the two values is mainly due to the incorrect calibration based on the alpha edges. This result emphasizes the importance of collecting good statistics in the region of highest lineal energy in order to allow for a more appropriate way of determining the edge as for instance, the second derivative method [28].

The DMD has been tested also under irradiation of 3.2 MeV neutron fields. The neutrons were produced by DD reaction at the Frascati Neutron Generator [29].

To calibrate the dosimeter in lineal energy, a spectrum with $^{241}\mathrm{Am}$ alpha source was collected before exposing the detector to the neutron beams, under the same working conditions. The response, recorded by the multichannel analyzer, is displayed in microdosimetric quantities in Fig. 11.

The neutron spectrum shows a small but significant edge at about $570\ \mathrm{keV}/\mu\mathrm{m}$ which overlaps the alpha edge of the calibration source. Moreover, a second edge is visible at approximately $200\ \mathrm{keV}/\mu\mathrm{m}$, compatible with the expected value of the proton edge in diamond (as for the alpha edge, the proton edge is the maximum energy that can be deposited by a proton in the sensitive volume).

This observation suggests the presence of alpha particles and protons produced by neutron reactions with elements of the detector and having energies sufficient to cross completely the sensitive volume.

Alpha particles with range in diamond up to $7.8\ \mu\mathrm{m}$ are produced by Boron doping through the reaction $^{10}\mathrm{B}(\mathrm{n},\alpha)^{7}\mathrm{Li}$ (Q-value 2.79 MeV and cross section around 300 mb), and protons with range in diamond up to $7.91\ \mu\mathrm{m}$ are produced in the reaction $^{27}\mathrm{Al}(\mathrm{n},\mathrm{p})^{27}\mathrm{Mg}$ (Q-value -1.83 MeV and cross section of 4–5 mb).

To conclude we recall that at the used neutron energies, carbon produces mainly elastic scattering and the energy deposition is due to carbon recoils. The measured spectra account for this effect in the lineal energy region $100-200\ \mathrm{keV}/\mu\mathrm{m}$, where a large number of events is measured compared to those due to the "edges" effect, from where most of the dose come from.

VI. Discussion

The feasibility of a diamond as microdosimeter is linked to the possibility of reducing the thicknesses of the detector to values of the order of the micrometer maintaining a well-defined sensing volume. A critical point, addressed in these first studies, concerns the definition of the sensing volume which in the internal side is defined by a doped boron layer. The distortion of the microdosimetric spectra would put in evidence non-uniform boron distributions caused by uncertainties on the definition of the thickness. The result of the experiments was encouraging, showing a good agreement between simulation and measurements which proves that the sensing volume is geometrically well defined also on the side of boron doping. In the case of standard dosimetry these distortions would be much less evident and harmful since the diamond sensing thickness is approximately 100 times larger and therefore the impact would be, in relative quantities, 100 times smaller.

Microdosimetry requires the acquisition of the single events of energy deposition. The presence of impurities on monocrystalline diamond would produce distortions on the collection of the signal, and the possibility of having for a single event of energy deposition, two distinguished signals due to the effect of the traps. The experimentally collected spectra showed no evidence of distortions which could be related to these phenomena. These effects cannot be "a priori" assumed from previous dosimetric measurements where multi-event energy depositions are collected and the effect of the charge traps is less relevant.

Finally, the reduced sizes of the microdosimeters show peculiar characteristics in terms of the electronic noise which in turn is linked, trough the feedback, to the intrinsic capacitance of the detector $(\mathrm{C_D})$. For a plane-parallel detector $\mathrm{C_D}$ is inversely proportional to the thickness of the detector itself. Therefore the decrease of the detector thickness (as necessary moving from dosimetry to microdosimetry) would proportionally increase the relative equivalent noise.

The microdosimeter described in the paper shows some preliminary yet encouraging results, confirming the potentialities of the use of CVD diamond in the specific field of microdosimetry. In particular, the agreement of the full width at half maximum of the experimental and simulated spectra (Fig. 9), shows no evidence of distortion due to non-uniform sensing volume definition or impurities. The compatibility of the nominal thickness with the thickness evaluated indirectly shows that the boron is well-distributed in the inner layer within an uncertainty of $\pm 1\ \mu\mathrm{m}$. With this first DMD prototype the collection of microdosimetric spectra in the region below $20\ \mathrm{keV}/\mu\mathrm{m}$ is unfeasible since the equivalent noise is about $4\ \mathrm{keV}/\mu\mathrm{m}$. This level of detector noise allows for good measurements of low energy (few MeV) alpha particles and protons, but gammas are not yet measurable.

A new set of diamond detectors will be developed shortly in which the capacitance of the sensing volume is decreased decreasing its transversal section.

VII. Conclusions

A preliminary study on a CVD diamond detector with micrometric sensitive volume has been carried out allowing the collection of spectra of energy deposition for alpha particles from

$^{241}\mathrm{Am}$ source and neutron beams of 3.2 MeV. The measurements pointed out the capability of the new DMD to discriminate the energy of densely ionizing radiation. Coupling the experimental data with the Monte Carlo calculation allows for a deeper understanding of the physical properties of the novel microdosimeter.

Numerical simulations of the DMD have been performed taking into account the influence of the dimension, shape and position of an aluminum collimator used to define the transversal side of the detector and increase the number of edge's events. The experimental spectrum of the $^{241}\mathrm{Am}$ alpha source (main energy 5.5 MeV) is in fair agreement with the Monte Carlo simulation. The main peak and edge positions are well reproduced and can be used to estimate the real thickness of the sensitive region. The difference between absolute numbers of events in the region $380 - 550\ \mathrm{keV}/\mu\mathrm{m}$ can be explained by a possible small discrepancy ($< 1\ \mathrm{mm}$) between the simulated position of the collimator compared to the real one.

The agreement between the experimental results and FLUKA Monte Carlo prediction provides insight about the physical behavior of the DMD and supports and strengthens the possibility of using this detector as a microdosimeter.

After this first analysis, systematic studies will be performed to investigate the detector response to other ionizing radiations including ions at accelerator facilities, gamma and X-rays. A redesign of the detector in order to increase the signal-to-noise-ratio (SNR) and to reduce the transversal sizes is in progress. The main goal is to extend its use to the rather demanding environment of particle therapy, where the spatial energy deposition patterns of the radiation fields are relevant for quantifying the resulting radiation damage in biological structures [30], [31]. Systematic studies will be performed to compare the results of the DMD to those of standard TEPCs.

REFERENCES

[1] P. M. Martineau *et al.*, "High crystalline quality single crystal chemical vapour deposit in diamond," *J. Phys.: Condens. Matter*, vol. 21, p. 364205, 2009.

[2] R. S. Balmer *et al.*, "Chemical vapour deposition synthetic diamond: Materials, technology and applications," *J. Phys.: Condens. Matter*, vol. 21, p. 364221, 2009.

[3] Y. Mokuno, A. Chayahara, and H. Yamada, "Synthesis of large single crystal diamond plates by high rate homoepitaxial growth using microwave plasma CVD and lift-off process," *Diam. Rel. Mater.*, vol. 17, p. 415, 2008.

[4] M. Marinelli, E. Milani, G. Prestopino, M. Scoccia, A. Tucciarone, G. Verona-Rinati, M. Angelone, D. Lattanzi, and M. Pillon, "High performance $^{6}\mathrm{LiF}$ diamond-thermal neutron detector," *Appl. Phys. Lett.*, vol. 89, p. 143509, 2006.

[5] M. Angelone, M. Pillon, M. Marinelli, E. Milani, G. Prestopino, A. Tucciarone, C. Verona, G. Verona-Rinati, I. Coffey, A. Murari, and N. Tartoni, "Single crystal artificial diamond detectors for VUV and soft X-ray s measurements on JET thermonuclear fusion plasma," *Nucl. Instrum. Meth. Phys. Res.*, vol. A623, pp. 726–730, 2010.

[6] M. Pillon, M. Angelone, A. Kràsa, A. J. M. Plompen, P. Schillebeeckx, and M. L. Sergi, "Experimental response functions of a single-crystal diamond detector for 5–20.5 neutrons," *Nucl. Instrum. Meth. Phys. Res.*, vol. A-640, pp. 185–191, 2011.

[7] S. Almaviva, M. Marinelli, E. Milani, G. Prestopino, A. Tucciarone, C. Verona, G. Verona-Rinati, M. Angelone, and M. Pillon, "Extreme UV single crystal diamond Schottky photodiode in planar traverse configuration," *Diam. Rel. Mater.*, vol. 19, p. 78, 2010.

[8] R. S. Wallny, "Status of diamond detectors and their high energy physics application," *Nucl. Instrum. Meth. Phys. Res.*, vol. A582, pp. 824–828, 2007.

[9] J. Field, Ed., The Proprieties of Diamond London, Academic Press, 1979.

[10] M. Angelone, M. Pillon, G. Prestopino, M. Marinelli, E. Milani, A. Tucciarone, C. Verona, G. Verona-Rinati, R. Bedogni, and A. Esposito, "Thermal and fast neutron dosimetry using artificial single crystal diamond detectors," *Rad. Meas.*, vol. 46, pp. 1686–1689, 2011.

[11] P. D. Bradley, A. B. Rosenfeld, K. K. Lee, D. Jamieson, G. Heiser, and S. Satoh, "Charge collection and radiation hardness of a SO1 microdosimeter for space and medical applications," *IEEE Trans. Nucl. Sci.*, vol. 45, pp. 2700–2710, 1998.

[12] J. A. Davis, K. Ganesan, S. Guatelli, M. Petasecca, J. Livingstone, D. A. Prokopovich, M. I. Reinhard, R. N. Siegele, S. Prawer, D. Jameson, Z. Kuncic, and A. B. Rosenfeld, "Characterization of a novel diamond-based microdosimeter for radioprotection applications in space environments," presented at the IEEE Symp. Nucl. Sci., Valencia, Spain, Oct. 2011.

[13] ICRU, Microdosimetry, Report 36 (Bethesda, MD: ICRU Publ.) 1983.

[14] A. J. Waker, "Principles of experimental microdosimetry," *Rad. Prot. Dosim.*, vol. 61, pp. 297–308, 1995.

[15] H. H. Rossi and W. Rosenzweig, "Measurements of neutron dose as a function of linear energy transfer," *Radiology*, vol. 64, pp. 404–411, 1955.

[16] P. D. Bradley, A. B. Rosenfeld, and M. Zaider, "Solid state microdosimetry," *Nucl. Instrum. Meth. Phys. Res.*, vol. B184, pp. 135–157, 2001.

[17] S. Agosteo and A. Pola, "Silicon microdosimetry," *Rad. Prot. Dosim.*, vol. 143, no. Issue2-4, pp. 409–415, 2011.

[18] M. Zaider, M. J. Bardash, and J. Ladik, "Solid state microdosimetry," *Rad. Prot. Dosim.*, vol. 85, pp. 443–446, 1999.

[19] H. H. Rossi, "Specification of radiation quality," *Radiat. Res.*, vol. 10, pp. 522–531, 1959.

[20] T. Loncol, V. Cosgrove, J. M. Denis, J. Gueulette, A. Mazal, H. G. Menzel, P. Pihet, and R. Sabattier, "Radiobiological effectiveness of radiation beams with broad LET spectra: Microdosimetric analysis using biological weighting functions," *Rad. Prot. Dosim.*, vol. 52, no. 1–4, pp. 347–352, 1994.

[21] A. M. Kellerer, "An assessment of wall effects in microdosimetric measurements," *Radiation Res.*, vol. 47, pp. 377–386, 1971.

[22] S. Almaviva, M. Marinelli, E. Milani, G. Prestopino, A. Tucciarone, C. Verona, G. Verona-Rinati, M. Angelone, M. Pillon, I. Dolbnya, K. Sawhney, and N. Tartoni, "Chemical vapor deposition diamond based multilayered radiation detector: Physical analysis of detection properties," *J. Appl. Phys.*, vol. 107, p. 014511, 2010.

[23] A. Ferrari, P. Sala, A. Fassò, and J. Ranft, "FLUKA: A Multi-Particle Transport Code" CERN-2005-10, INFN/TC_05/11, SLAC-R-773, 2005.

[24] G. Battistoni, S. Muraro, P. R. Sala, F. Cerutti, A. Ferrari, S. Roesler, A. Fassò, and J. Ranft, M. Albrow and R. Raja, Eds., "The FLUKA code: Description and benchmarking," in *Proc. Hadronic Shower Simulation Workshop, Fermilab AIP Conf.*, Sep. 2007, vol. 896, pp. 31–49.

[25] [Online]. Available: http://physics.nist.gov/PhysRefData/Star/Text/ASTAR.html

[26] A. Rytz, "Recommended energies and intensity values of alpha particles from radioactive decay," *Atomic Data Nucl. Data Tables*, vol. 47, no. 2, pp. 205–239, 1991.

[27] S. Gerdung, P. Pihet, J. E. Grindborg, H. Roos, U. J. Schrewe, and H. Schuhmacher, "Operation and application of tissue equivalent proportional counters," *Rad. Prot. Dosim.*, vol. 61, no. 4, pp. 381–404, 1995.

[28] L. De Nardo, V. Cesari, G. Doná, G. Magrin, P. Colautti, V. Conte, and G. Tornielli, "Mini-TEPCs for radiation therapy," *Rad. Prot. Dosim.*, vol. 108, no. 4, pp. 345–352, 2004.

[29] M. Martone, M. Angelone, and M. Pillon, "The 14 MeV Frascati neutron generator," *J. Nucl. Mater.*, vol. 63, pp. 1661–1663, 1993.

[30] S. Rollet, P. Colautti, B. Grosswendt, J. Herault, M. Wind, E. Gargioni, P. Beck, M. Latocha, and D. Moro, "Microdosimetric assessment of the radiation quality of a therapeutic proton beam: Comparison between numerical simulation and experimental measurements," *Rad. Prot. Dosim.*, vol. 143, no. 2–4, pp. 445–449, 2011.

[31] T. T. Böhlen, M. Dosanjh, A. Ferrari, I. Gudowska, and A. Mairani, "FLUKA simulations of the response of tissue-equivalent proportional counters to ion beams for applications in Hadron therapy and space," *Phys. Med. Biol.*, vol. 56, pp. 6545–6561, 2011.